VIBRATIONS OF SHAFT CAUSED BY INERTIAL EXCITATIONS

Anastas I. Ivanov

Todor Kableshkov Higher School of Transport, 1574 Sofia; aii2010@abv.bg

ABSTRACT. Small vibrations of a cylindrical shaft caused by inertial excitations are studied in this paper. The shaft is vertically situated. It consists of two sections with different cross sections. It is supported by a spherical and a cylindrical joint. The two supporting devices have horizontal elasticity. Between the two supports, and also at the upper end of the shaft, rotationally movable concentric masses, which are eccentrically situated towards the shaft axis, are mounted. They rotate with a constant angular velocity relative to the rotary axis and they create unfavourable inertial excitations. Due to the elasticity of the shaft, as well as to the elastic horizontal supports, small forced vibrations of the two concentric masses are created in planes perpendicular to the rotary axis. The shaft is modelled as a discrete mechanical system with four degrees of freedom. Differential equations, describing the small vibrations of the system, are derived. A programme of MatLab and Simulink has been compiled and used to integrate numerically derived equations. Calculations have been made for the different unfavourable positions of the concentrated masses relative to a plane perpendicular to the shaft rotary axis. All results are illustrated with appropriate graphs. Some important for the practice conclusions are presented, which can be used in the design of such shafts.

Keywords: shaft, vibrations, inertial excitations, kinematical characteristics

ТРЕПТЕНИЯ НА ВАЛ, ПРЕДИЗВИКАНИ ОТ ИНЕРЦИОННИ СМУЩЕНИЯ

Анастас И. Иванов

Висше транспортно училище "Тодор Каблешков", 1574 София

РЕЗЮМЕ. В статията се изследват малките трептения на цилиндричен вал, предизвикани от инерционни смущения. Валът е разположен вертикално. Състои се от два участъка с различни по размер напречни сечения. Подпрян е със сферична и цилиндрична става. Двете опорни устройства имат хоризонтална еластичност. Между тях, и в най-горния край на вала, са монтирани ротационно движещи се спрямо оста му ексцентрично разположени концентрирани маси. Те се въртят с постоянна ъглова скорост спрямо ротационната ос и създават неблагоприятни инерционни смущения. Поради еластичността на вала, както и поради еластичните в хоризонтално направление опори, се пораждат малки принудени трептения на двете концентрирани маси в равнини, перпендикулярни на ротационната ос. Валът е моделиран като дискретна механична система с четири степени на свобода. Изведени са диференциалните уравнения, които описват малките трептения на системата. Съставена е програма на MatLab и Simulink, с помощта на която са интегрирани числено изведените уравнения. Извършени са изчисления за неблагоприятните взаимни разположения на концентрираните маси спрямо равнина перпендикулярна на оста на вала. Всички резултати са онагледени с подходящи графики. Статията завършва с важни за практиката изводи, които могат да се използват при проектирането на подобен вид валове.

Ключови думи: Вал, трептения, инерционни смущения, кинематични характеристики

Introduction

Many machines and aggregates use different types of shafts. Most often they are examined for torsion and bending because their main purpose is to transmit axial moments (Sevastakiev et al., 1986).

In the presented article, the shaft is examined only on a generalised bending caused by inertial harmonic excitations. Such disturbances are always presented in the rotary machines when unbalanced masses are available (Sergeev et al., 2018).

Harmful vibrations, which are small oscillations with high frequencies and relatively small amplitudes, accompany each machine aggregate as crushers, mills and others (Hristova, et al., 2018). Reducing them to some minimal normative values is the most important engineering problem for solving by any constructor (Petrović, 2017; Sergeev et al., 2018).

For example, the three-dimensional vibrations of a machine aggregate, solved numerically with a suitable program for this purpose, are studied in the paper (Ivanov, 2017).

One of the most important and basic task, the determination of eigen frequencies and eigen forms, is very difficult to solve using only analytical solutions, especially for the systems with many degrees of freedom, (Ivanov, 2017). The engineer needs to make many calculations numerically for multiple variants, which are dependent on a number of parameters. Only then, the optimisation analysis can be made (Cheshankov et al., 2004).

The above-mentioned problems lead to the compilation of the main purpose of this study: to determine the maximum values of the basic kinematical characteristics of a vertical shaft from the most unfavourable inertial excitation.

Mathematical model

A vertically positioned cylindrical shaft, which has two sections, is studied.

The first section has a length l_1 and bending stiffness $E.I_1$, and the second section has length l_2 and bending stiffness $E.I_2$, (Fig. 1).

The shaft is supported at its lower end by a spherical joint, which is equivalent to three simple rod joints. The vertical rod joint is assumed to be perfectly rigid. The two mutually perpendicular and horizontal rod joints are assumed to be ideally elastic with linear stiffness coefficients c_1.

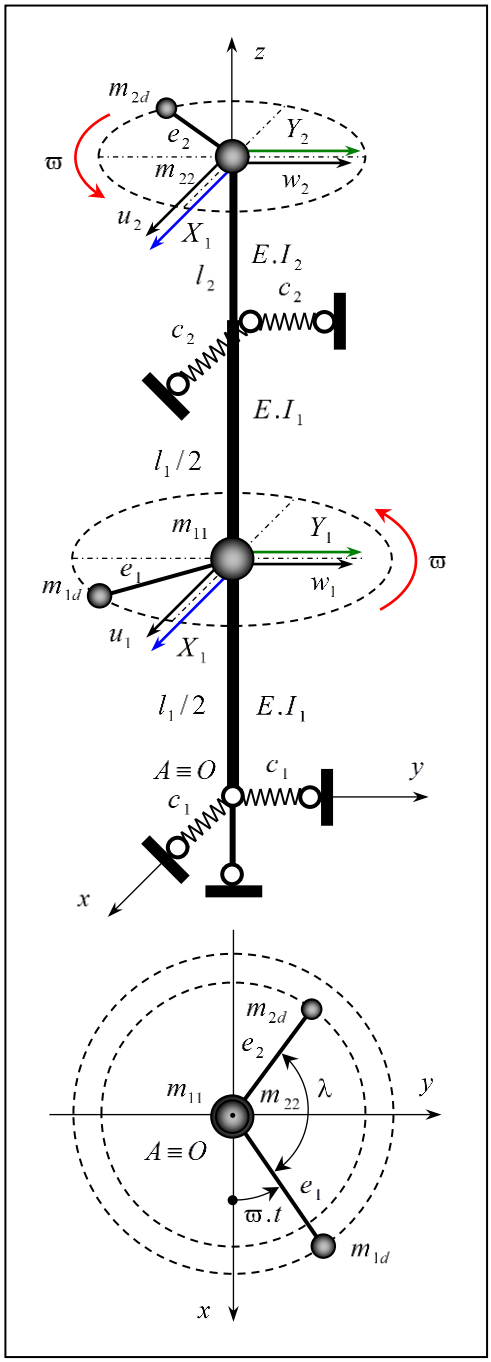

Fig. 1. Dynamical model of the shaft

At the end of the first section and at the beginning of the second one, the shaft is supported by a cylindrical joint. It is equivalent to two horizontal rod joints, which are assumed to be ideally elastic with linear stiffness coefficients c_2.

In the middle of the first section are centrally located a concentrated mass m_{11} and an unbalanced mass m_{1d}, and $m_1 = m_{11} + m_{1d}$. The unbalanced mass m_{1d} is located at a distance e_1 from the shaft axis.

At the upper end of the shaft are centrally located a concentrated mass m_{22} and an unbalanced mass m_{2d} with an eccentricity e_2, and $m_2 = m_{22} + m_{2d}$.

The two unbalanced masses rotate synchronously around the rotary axis Oz with the same angular velocity ϖ and phase difference λ.

Differential equations

The vector of the generalised coordinates, which are determined by the small vibrations of the discrete mechanical system, has the type (Fig. 1):

$$\mathbf{q} = \left\langle u_1 \quad u_2 \quad w_1 \quad w_2 \right\rangle^T . \tag{1}$$

The Lagrange differential equations of second gender are used. They have the following matrix form:

$$\frac{\partial}{\partial t}\left(\frac{\partial E_k}{\partial \dot{\mathbf{q}}}\right) - \left(\frac{\partial E_k}{\partial \mathbf{q}}\right) = \mathbf{Q} - \frac{\partial E_p}{\partial \mathbf{q}} . \tag{2}$$

The kinetic energy of the system is a quadratic form of the vector generalised velocities and the mass matrix:

$$E_k = 0{,}50 . \dot{\mathbf{q}}^T . \mathbf{M} . \dot{\mathbf{q}} , \tag{3}$$

$$\mathbf{M} = \mathbf{diag}\left(m_1 \quad m_2 \quad m_1 \quad m_2\right). \tag{4}$$

The potential energy of the deformations is the quadratic form of the vector of generalised coordinates and the stiffness matrix:

$$E_p = 0{,}50 . \mathbf{q}^T . \mathbf{K} . \mathbf{q} , \tag{5}$$

$$\mathbf{K} = \begin{bmatrix} k_{11} & k_{12} & 0 & 0 \\ k_{21} & k_{22} & 0 & 0 \\ 0 & 0 & k_{11} & k_{12} \\ 0 & 0 & k_{21} & k_{22} \end{bmatrix} . \tag{6}$$

The determination of the stiffness matrix is done by the mathematical dependence:

$$\mathbf{K} = \mathbf{D}^{-1} , \tag{7}$$

where the flexibility matrix has the form:

$$\mathbf{D} = \begin{bmatrix} d_{11} & d_{12} & 0 & 0 \\ d_{21} & d_{22} & 0 & 0 \\ 0 & 0 & d_{11} & d_{12} \\ 0 & 0 & d_{21} & d_{22} \end{bmatrix} , \tag{8}$$

$$d_{11} = \frac{l_1^3}{48.E.I_1} + \frac{c_1 + c_2}{4.c_1.c_2} \ , \tag{9}$$

$$d_{22} = \frac{l_1.l_2^2}{3.E.I_1} + \frac{l_2^3}{3.E.I_2} + \\ + \frac{l_2^2}{l_1^2}.\frac{c_1 + c_2}{c_1.c_2} + \frac{l_1 + 2.l_2}{l_1}.\frac{1}{c_2} \ , \tag{10}$$

$$d_{12} = d_{21} = -\frac{l_1^2.l_2}{16.E.I_1} - \frac{l_2}{2.l_1}.\frac{1}{c_1} + \frac{l_1 + l_2}{2.l_1}.\frac{1}{c_2} \ . \tag{11}$$

The vector of the generalised non-potential forces is formed by the inertial forces that arise in the two unbalanced masses. This vector has the type:

$$\mathbf{Q} = \left\langle X_1 \quad X_2 \quad Y_1 \quad Y_2 \right\rangle^T \ , \tag{12}$$

$$X_1 = m_{1d}.e_1.\varpi^2.\cos(\varpi.t) \ , \tag{13}$$

$$X_2 = m_{2d}.e_2.\varpi^2.\cos(\varpi.t + \lambda_n) \ , \tag{14}$$

$$Y_1 = m_{1d}.e_1.\varpi^2.\sin(\varpi.t) \ , \tag{15}$$

$$Y_2 = m_{2d}.e_2.\varpi^2.\sin(\varpi.t + \lambda_n) \ . \tag{16}$$

The system of differential equations, which describes the small vibrations of the two concentrated masses recorded in a matrix form, has the following type:

$$\mathbf{M}.\ddot{\mathbf{q}} + \mathbf{K}.\mathbf{q} = \mathbf{Q} \ . \tag{17}$$

The upper differential equation system (17) is linear, non-homogeneous, from the second order and it is composed of constant coefficients. It could be integrated analytically (Ivanov, 2017). But when multiple engineering calculations are performed with variations of many parameters, it is advisable to solve it numerically with a suitable program. It can be compiled on the basis of some powerful mathematical package.

Numerical solution

For the numerical solution of the differential equation system (17) in the time area, the MatLab ver. 6.1 and Simulink Toolbox are used.

Eigen frequencies

In order to avoid the dangerous resonance areas, the eigen frequencies were primarily determined.

This task is related to defining the own numbers of the matrix $\mathbf{A}$, which has the following structure:

$$\mathbf{A} = \begin{bmatrix} \mathbf{0} & \mathbf{I} \\ -\mathbf{M}^{-1}.\mathbf{K} & \mathbf{0} \end{bmatrix}_{8\times 8} \ . \tag{18}$$

Sub-matrices $\mathbf{0} = [0]_{4\times 4}$ and $\mathbf{I} = \mathbf{diag}[1]_{4\times 4}$ are correspondingly zero and unit matrices.

The eigen circular frequencies ω_k, $(k = 1,2,3,4)$, are derived from the own numbers p_k that have the form:

$$p_k = 0 \pm i.\omega_k \ , \qquad i = \sqrt{-1} \ . \tag{19}$$

Initially, a program file "shaft.m" is created. Then this file is started from the MatLab main command window.

Simulink model file

Initially, the differential equations (17) are presented in the following matrix form:

$$\ddot{\mathbf{q}} = \left[-\mathbf{M}^{-1}.\mathbf{K} \quad \mathbf{0} \right].\begin{bmatrix} \mathbf{q} \\ \dot{\mathbf{q}} \end{bmatrix} + \mathbf{M}^{-1}.\mathbf{Q} \ . \tag{20}$$

A model simulation file "shaft.mdl" is created. This file is started from the Simullink command window.

Numerical results

In order to avoid dangerous resonance areas, the eigen frequencies were originally determined.

The calculations are made using the following numerical parameters:

$E = 2.10^{11}\ Pa$, $m_{11} = 598\ kg$, $m_{22} = 399\ kg$,

$m_{1d} = 2\ kg$, $m_{2d} = 1\ kg$, $c_1 = 5.10^4\ N/m$,

$c_2 = 8.10^4\ N/m$, $I_1 = 1,6.10^{-6}\ m^4$, $I_2 = 0,8.10^{-6}\ m^4$,

$l_1 = 6\ m$, $l_2 = 2\ m$, $e_1 = 0,08\ m$, $e_2 = 0,06\ m$,

The following values of the eigen circular frequencies are obtained:

$\omega_1 = 5,997\ s^{-1}$, $\omega_2 = 5,997\ s^{-1}$, $\omega_3 = 9,147\ s^{-1}$,

$\omega_4 = 9,147\ s^{-1}$.

The safe frequency areas of the forced circular frequency ϖ for avoidance of resonant phenomena are: $\varpi \le 4\ s^{-1}$ as well as $\varpi \ge 12\ s^{-1}$.

Forced circular frequency $\varpi = 40\ s^{-1}$ is accepted.

The system of differential equations (20) is integrated with a variable step by the selected method ode 113 (Adams) and maximum time duration $t = 5\ s$.

The calculations are made for thirteen values of the phase difference λ_n, namely $\lambda_n = n.\pi/12\ rad$, $(n = 0,1,2,...,11,12)$.

For each phase difference λ_n, the magnitudes of the displacement of the two masses m_1 and m_2 are determined using the following formulas:

$$A_{1n} = \sqrt{u_{1n}^2 + w_{1n}^2} \ , \qquad A_{2n} = \sqrt{u_{2n}^2 + w_{2n}^2} \ . \tag{21}$$

For the first mass m_1, the maximum deviation from the shaft axis is obtained with a phase difference $\lambda_0 = 0.\pi/12\ rad$, and it has a value $A_{10} = 0,00164\ m$.

For the second mass m_2, the maximum deviation from the axis is obtained with a phase difference $\lambda_{11} = 11.\pi/12\ rad$, and it has a value $A_{211} = 0,002027\ m$.

The graphs of functions $A_{10} = A_{10}(t)$ and $A_{211} = A_{211}(t)$ are shown in Figure 2 and Figure 3, respectively.

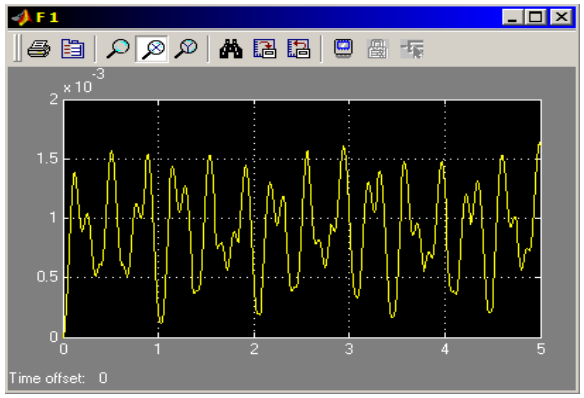

Fig. 2. Displacement of the first mass during the integration time

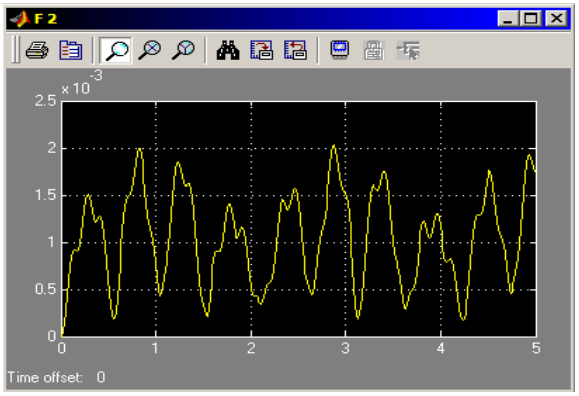

Fig. 3. Displacement of the second mass during the integration time

The prepared model file allows the trajectory traces of each mass in a horizontal plane parallel to the plane Oxy to be visualised.

These trajectory traces of the two masses for the same unfavourable phase differences are shown in Figure 4 and Figure 5, respectively.

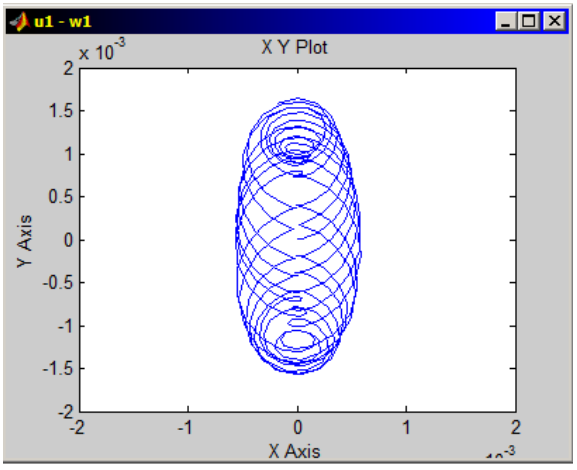

Fig. 4. Trajectory trace of the first mass in the horizontal plane

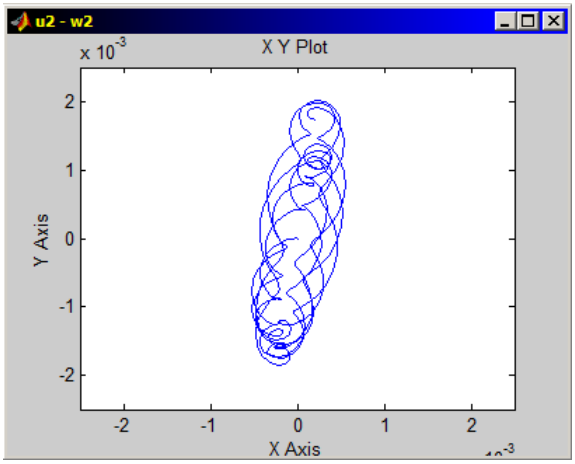

Fig. 5. Trajectory trace of the second mass in the horizontal plane

A study has also been done for the maximum velocities and the maximum accelerations of the two masses.

For each phase difference λ_n the velocity v_n and acceleration a_n of the two masses m_1 и m_2 are determined by the formulas:

$$v_{1n} = \sqrt{\dot{u}_{1n}^2 + \dot{w}_{1n}^2}\ , \qquad v_{2n} = \sqrt{\dot{u}_{2n}^2 + \dot{w}_{2n}^2}\ , \tag{22}$$

$$a_{1n} = \sqrt{\ddot{u}_{1n}^2 + \ddot{w}_{1n}^2}\ , \qquad a_{2n} = \sqrt{\ddot{u}_{2n}^2 + \ddot{w}_{2n}^2}\ . \tag{23}$$

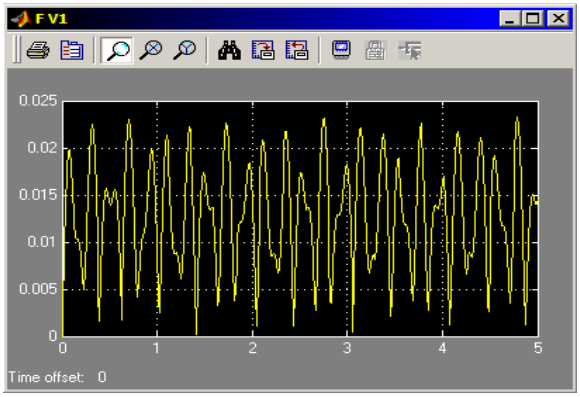

Fig. 6. Velocity of the first mass during the integration time

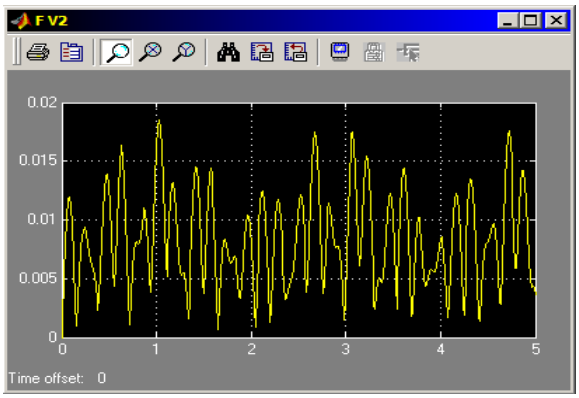

Fig. 7. Velocity of the second mass during the integration time

For the first mass m_1, the maximum velocity is obtained with a phase difference $\lambda_0 = 0.\pi/12\ rad$, and it has a value $v_{10} = 0,0233\ m/s.$

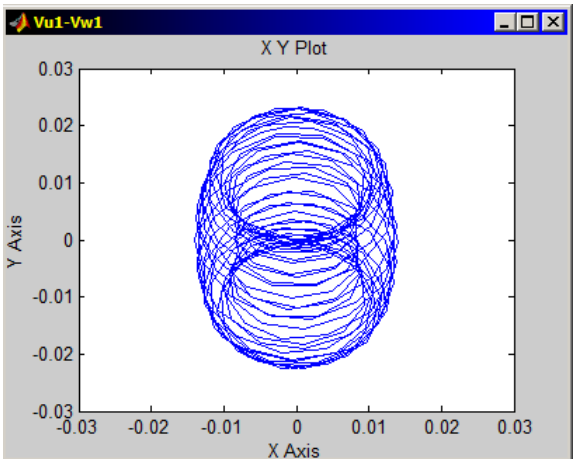

Fig. 8. A trace of velocity vector peak of the first mass in the horizontal plane

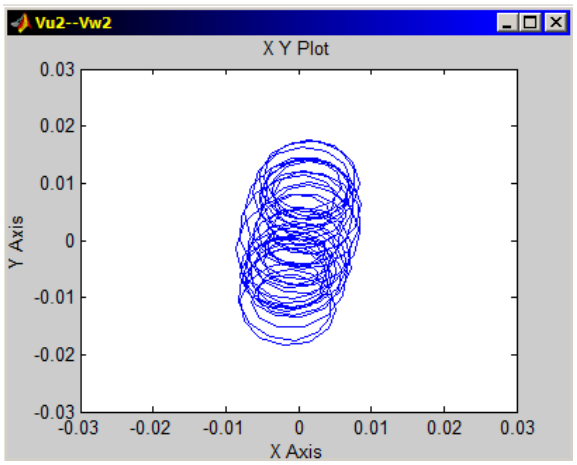

Fig. 9. A trace of velocity vector peak of the second mass in the horizontal plane

For the second mass m_2, the maximum velocity is obtained with a phase difference $\lambda_{11} = 11.\pi/12\ rad$ and it has a value $v_{211} = 0,0185\ m/s.$

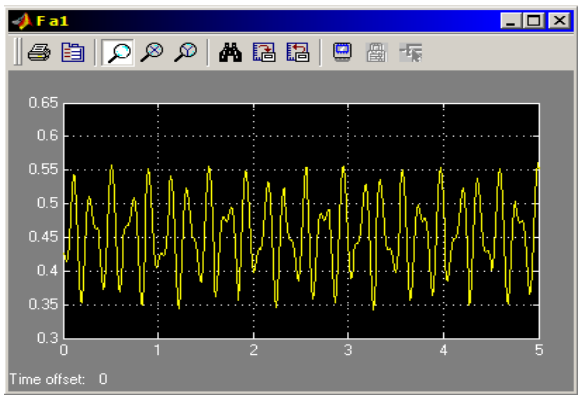

Fig. 10. Acceleration of the first mass during the integration time

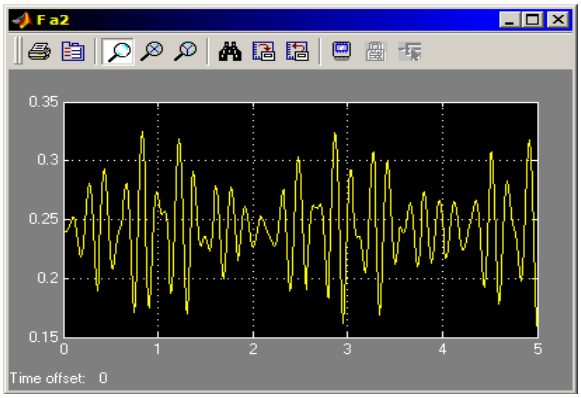

Fig. 11. Acceleration of the second mass during the integration time

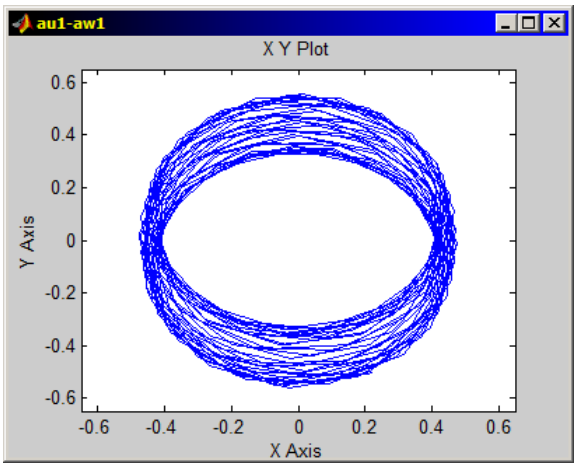

Fig. 12. A trace of acceleration vector peak of the first mass in the horizontal plane

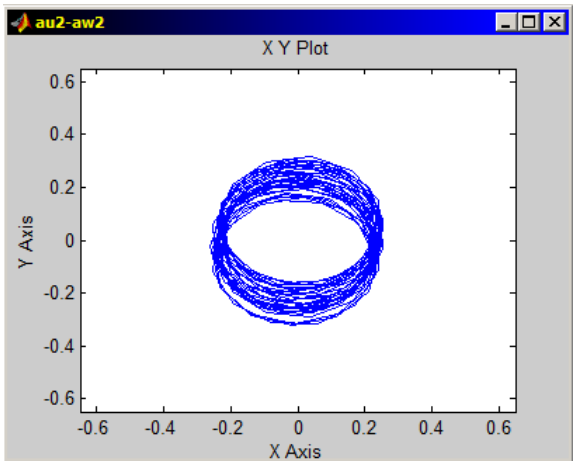

Fig. 13. A trace of acceleration vector peak of the second mass in the horizontal plane

The graphs of functions $v_{10} = v_{10}(t)$ and $v_{211} = v_{211}(t)$ are shown in Figure 6 and Figure 7, respectively.

The trace of velocity vector peaks of the two masses for the correspondingly unfavourable mutual positions are shown in Figure 8 and Figure 9, respectively.

For the first mass m_1, the maximum acceleration is obtained with a phase difference $\lambda_0 = 0.\pi/12\ rad$, and it has a value $a_{10} = 0,5606\ m/s^2$.

For the second mass m_2, the maximum acceleration is obtained with a phase difference $\lambda_{11} = 11.\pi/12\ rad$ and it has a value $a_{211} = 0,3236\ m/s^2$.

The graphs of functions $a_{10} = a_{10}(t)$ and $a_{211} = a_{211}(t)$ are shown in Figure 10 and Figure 11, respectively.

The trace of acceleration vector peaks of the two masses for the correspondingly unfavourable mutual positions are shown in Figure 12 and Figure 13, respectively.

Conclusion

The main issue is solved.

1. An application program in the area of MatLab ver. 6.1 and in the area of Simulink Toolbox for numerical calculation of free and forced vibrations of a mechanical system with four degrees of freedom is compiled and adapted to this task.
2. The eigen frequencies of this mathematical model of the shaft are determined, and based on these values, a forced circular frequency is selected which is outside the resonant danger zone.
3. The maximum values of the displacements, velocities and accelerations of the two concentrated masses at the correspondingly the most unfavourable mutual position of the two unbalanced masses are determined.
4. All calculated kinematical characteristics are illustrated in detail in Figures 2 to13.
5. This study shows the advantages of the numerical solution compared to the respective analytical solution. These advantages could be summarised as follows:

- Ability to change many input parameters and calculate many variants for a relatively short machine time (Stoyanov, 2018; Stoyanov, 2017).
- Ability to optimise input parameters and the final results using Toolbox Optimisation (Tonchev et al., 2013).

This task provides the basis for further research, complicating the model with the following additions:

1. To take into account the damping in the system.
2. To take into account the effect of horizontal kinematical disturbances that could occur in both supports.
3. To take into account the influence of the distributed mass on the two shaft sections at the bending study.
4. To complicate the dynamical model, taking into account the twist and total bending of the shaft in the two mutually perpendicular planes.

The solved task could be used at the construction of aggregates in the mining industry.

It is also useful for Bachelors, Masters and PhD students who study the Theory of Mechanisms and Machines and Vibrations in Techniques (Sergeev et al., 2018).

The article shows a modern numerical study with the MatLab package (Ivanov, 2011). Such studies can also be performed with other MatLab toolboxes (Marinov et al., 2016), as well as with other mathematical packages such as MathCAD (Stoyanov, 2017, Stoyanov, 2017).

References

Cheshankov B., I. Ivanov, V. Vitliemov, P. Koev. 2004. PCI-method multi-criteria optimisation contracting the set of trade-off solutions. – *15th International Conference on Systems Science*, Wrozlaw, 1–8.

Hristova T. V., A. B. Yanev, N. V. Savov. 2018. Determination of the influence of jaw movement frequency of jaw crusher on energy consumption. – *Annual of the University Petroşani, Electrical Engineering, 20*, 29–36.

Ivanov, A. 2017. Vliyanie na disipaciyata pri izsledvane na svobodnite prostranstveni trepteniya na tvardo tyalo. – *Proceedings of the Annual University Scientific Conference.* Vasil Levski National Military University, Veliko Tarnovo, 234–243 (in Bulgarian with English abstract).

Ivanov, A. 2011. *Modelirane na dinamichni zadachi s MATLAB*. Avangard Prima, Sofia, 100 p. (in Bulgarian)

Ivanov, A. 2017. Three dimensional vibrations of aggregate connected with elastic elements. – *Technomus Journal*, Suceava, 37–42.

Marinov, M., G. Nikolov, E. Gieva, B. Ganev. 2016. Environmental Noise Logging and Calculating. – *IEEE, 39th International Spring Seminar on Electronics Technology (ISSE)*, 425–429.

Petrović, D., M. Bižić, D. Atmadzhova, 2017. Application of rubber elastic elements in suspension of railway vehicles. – *Journal Mechanics, Transport, Communications*, *15*, 3, № 1490. VI-44–VI-51.

Sergeev, Yu. S., S. V. Sergeev, A. A. Dyakonov, E. N. Gordeev. 2018. Improving geometric homogeneity of particles crushed using vibrational drive with modulating properties in machine for crushing brittle materials. – *Journal of Advanced Research in Dynamical and Control Systems*, *13 Special Issue*, 2411–2422.

Sergeev, Yu. S., S. V. Sergeev, A. A. Dyakonov, A. V. Kononistov, G. E. Karpov, A. A. Mikryukov. 2018. Automated monitoring system for self-synchronizing vibrational drives. – *Russian Engineering Research*, *38*, 2, 86–90.

Sergeev, S. V., Yu. S. Sergeev, A. V. Kononistov. 2018. Self-synchronized controlled vibration drive with automated oscillation parameters monitoring system for high-tech equipment. – *ICIE 2018: Proceedings of the 4th International Conference on Industrial Engineering*, 367–374.

Sevastakiev, V., V. Zhivkov, E. Marinov. 1986. *Dinamika i trepteniya na dvigateli s vatreshno gorene*. Tehnika, Sofia, 414 p. (in Bulgarian)

Stoyanov, A. 2017. Solving of statically determined plane truss not built from triangles. – *International Journal of Advancement in Engineering Technology, Management and Applied Sciences (IJAETMAS)*, *4*, 7, 13–22.

Stoyanov, A. 2017. The equilibrium of a body loaded with a spatial system of forces. – *Journal of Mining and Geological Sciences*, *60*, 77–81.

Stoyanov, A. 2017. Research of the equilibrium of a spatial truss with the programming system MathCAD. – *Proceedings of the Annual University Scientific Conference*, Vasil Levski National Military University, Veliko Tarnovo, 214–221 (in Bulgarian with English abstract).

Stoyanov, A. 2018. The movement of a point set in Cartesian coordinates and studied in the MathCAD environment. *Journal of Mining and Geological Sciences*, *61*, 64–69.

Tonchev, Y., V. Vitliemov. 2013. *Optimizaciya s MATLAB. Pragmatichen podhod*. Publising “Angel Kanchev”, Rousse, 250 p. (in Bulgarian)